



EUROPEAN ORGANIZATION FOR NUCLEAR RESEARCH

CERN-EP/83-152

3 October 1983

A SEARCH FOR ν_μ OSCILLATIONS IN THE Δm^2 RANGE 0.3 TO 90 eV²

F. Dydak, G.J. Feldman^{*)}, C. Guyot, J.P. Merlo, H.-J. Meyer^{**)}, J. Rothberg^{***)}, J. Steinberger,
H. Taureg, W. von Rüden, H. Wachsmuth, H. Wahl and J. Wotschack
CERN, Geneva, Switzerland

H. Blümer, P. Buchholz, J. Duda, F. Eisele, K. Kleinknecht, J. Knobloch, B. Pszola and B. Renk
Institut für Physik der Universität, Dortmund, Fed. Rep. Germany^{†)}

R. Belusevic, B. Falkenburg, T. Flottmann, J.G.H. de Groot, C. Geweniger,
H. Keilwerth and K. Tittel
Institut für Hochenergiephysik der Universität, Heidelberg, Fed. Rep. Germany^{†)}

P. Debu, A. Para, P. Perez, B. Peyaud, J. Rander, J.P. Schuller and R. Turlay
DPhPE, CEN-Saclay, France

H. Abramowicz and J. Królikowski
Institute of Experimental Physics, Warsaw University, Poland

ABSTRACT

We have searched for ν_μ oscillations by comparing the rates of ν_μ charged-current interactions in two detectors located 130 and 885 m from the target, which was struck by a 19.2 GeV/c proton beam from the CERN Proton Synchrotron. No evidence for ν_μ oscillations was found. At the 90% confidence level, Δm^2 values between 0.26 and 90 eV² are excluded for maximal mixing. The most restrictive limit on the neutrino mixing-angle parameter $\sin^2 2\Theta$ is 0.053 at $\Delta m^2 = 2.5$ eV².

(Submitted to Physics Letters)

^{*)} On leave from SLAC, Stanford University, Calif., USA.

^{**)} On leave from the Universität-Gesamthochschule Siegen, Fed. Rep. Germany.

^{***)} Visitor from the University of Washington, Seattle, USA.

^{†)} Supported by the Bundesministerium für Forschung und Technologie, Bonn, Fed. Rep. Germany.

If different neutrino species have different masses, it is possible that the neutrino-mass eigenstates will not coincide with the eigenstates of the weak interactions. In this case, a neutrino produced in a weak interaction will appear to evolve with time into a linear combination of weak eigenstates [1]. Here we report a search for such a phenomenon by comparing the rate of ν_μ charged-current interactions in two detectors, each at a different distance from the target.

Previously published searches for ν_μ oscillations have sought to measure the anomalous appearance of ν_e or ν_τ charged-current interactions [2–5]. The present experiment, by measuring the disappearance of muon-neutrinos, goes beyond the previous work in several ways: it is sensitive to oscillations of ν_μ to neutrinos of fourth or higher generations; it is sensitive to $\nu_\mu \leftrightarrow \nu_\tau$ oscillations at energies below threshold for τ^\pm production; and, in some regions, it is also more sensitive to $\nu_\mu \leftrightarrow \nu_e$ oscillations than the earlier experiments.

For simplicity we assume that the ν_μ is primarily a linear combination of two mass eigenstates,

$$\nu_\mu = \nu_1 \cos \Theta + \nu_2 \sin \Theta. \quad (1)$$

Then the probability that a ν_μ will remain a ν_μ at a distance L from its production point is

$$P(\nu_\mu \rightarrow \nu_\mu) = 1 - \sin^2 2\Theta \sin^2(1.27 \Delta m^2 L/E_\nu), \quad (2)$$

where L is in metres, E_ν is the ν energy in MeV, and $\Delta m^2 = |m_{\nu_1}^2 - m_{\nu_2}^2|$ is the absolute value of the difference of the masses squared of the two neutrino-mass eigenstates, ν_1 and ν_2 , in eV^2 .

The objective of the experiment was to be sensitive to a value of Δm^2 as low as possible. This required low neutrino energies and at the same time large distances L between the neutrino source and the detector. A further constraint was to use, in part, the existing CDHSW detector, which is located in the CERN Super Proton Synchrotron (SPS) neutrino beam. For this reason, a new PS neutrino beam line was constructed, pointing towards the existing detector located 885 m from the proton target (see fig. 1a). In order not to be dependent on the absolute neutrino flux, a second detector, constructed with modules identical in design to those in the existing detector, was placed 130 m from the target; data were taken simultaneously by the two detectors.

Protons of 19.2 GeV/c were used to form the neutrino beam. The target was a beryllium rod, 60 cm long and 8 mm in diameter. The decay tunnel was 52 m long, followed by 4 m of iron and 70 m of molasse to absorb the muons. The neutrino flux peaked around 1 GeV, and dropped proportionally to e^{-E_ν} at higher energies. No magnetic focusing was done behind the target. The divergence of the neutrino beam was therefore much larger than the solid angle of either detector, so that in the absence of oscillations the ν_μ flux scaled as approximately L^{-2} .

The layout of the experiment is shown in fig. 1b. The two detectors were aligned at the same horizontal and vertical angles to the ν beam, 384 mrad and 30 mrad respectively. The front detector was centred on the beam line, whilst the back detector, covering a smaller solid angle, was centred on the average angle subtended by the front detector in order to better sample the same ν energy spectrum.

Each detector consists of three distinct types of modules, all of them being sandwiches of circular, 3.75 m diameter, iron plates and plastic scintillator hodoscopes, and having the following characteristics.

Type I has 2.5 cm thick iron plates and 15 cm wide scintillators. A single module consists of

20 iron and scintillator planes. Each set of five scintillators, aligned alternately to view the horizontal and the vertical position, is read in depth by a single photomultiplier. Thus the thickness of iron per module is 50 cm with four readings in depth and an effective transverse granularity of 15×15 cm.

The type II modules [6] have 5 cm iron sampling and 45 cm wide scintillators, each scintillator being read by two photomultipliers. All the scintillators are arranged to measure the vertical position only. Each module corresponds to 75 cm of iron with 15 samplings in depth.

The type III modules are similar to type II except that they have only five planes of iron, each 15 cm thick.

The back detector (at 885 m) is composed of ten type I modules, five type II modules, and six type III modules, whilst the front detector (at 130 m) consists of two modules of each type. Because of the low energy of the events in this experiment, the iron plates were not magnetized and the drift chambers between modules were not used. The trigger was based on the projected range of iron traversed by the most penetrating particle of the event. Trigger planes were constructed by adding all the signals from single hodoscope planes in the type I modules and from groups of three consecutive scintillator planes in the type II modules. The type III modules were not used in the trigger. Events were recorded in which three out of any four adjacent trigger planes had a pulse height greater than 20% of that caused by a minimum ionizing particle. The minimal "length" of an event is therefore required to be about 30 cm of iron.

The data reported here correspond to 7×10^{18} protons on target. Typically the experiment received 1.1×10^{13} protons per $2.1 \mu\text{s}$ spill with a repetition rate of 1.2 s. Data were acquired in a $3 \mu\text{s}$ gate centred around the beam spill and in a $600 \mu\text{s}$ gate outside the spill. Events recorded during this gate were used to measure the cosmic-ray background and to monitor the apparatus performance. Typical event rates were 1/6 and 1/70 beam correlated events per 10^{13} protons in the front and the back detector, respectively. The corresponding cosmic-ray rates per burst were 1/250 and 1/60. These data rates gave rise to dead-times of $(9 \pm 1)\%$ and $(2 \pm 0.2)\%$.

An off-line analysis program determined a vertex and a muon direction for each event. To eliminate most of the cosmic-ray background, events were required to have a vertical angle of less than 45° with respect to the axis of the detector, and not to enter through the top of the detector. To eliminate particles from neutrino interactions outside the detector, events were rejected if they appeared to originate in the first plane of the detector, or at a radius of greater than 1.6 m in the type I modules, or in the top or bottom scintillator of the type II modules. Since the type II modules provided no horizontal position information, a large plane of scintillators was installed as an anticounter in front of each of these modules on the side of the detector facing the beam (see fig. 1b). Events were rejected if there was a signal in the anticounter immediately preceding the module which appeared to contain the event vertex.

Several steps were taken to ensure that as similar an analysis as possible was performed in the two detectors, the principal difference between them being that the front detector was shorter than the back detector. First, events were characterized by whether they originated in modules of type I or II. Ratios of rates in the back detector to those in the front detector were formed separately for the two types of modules.

Secondly, a fiducial volume for the event vertex was defined to contain an integral number of modules in each detector so that acceptance differences depending on the relative vertex position within a module were minimized. For each type of module the fiducial volume extended from the

second plane of the first module to the first plane of the last module. In this way events which started near the boundary between two types of modules were rejected, the relative number of such events being different in the two detectors. Thus the fiducial volume for the event vertex was equivalent to nine modules of type I and four modules of type II in the back detector and one of each type in the front detector.

Finally, events were classified according to their range in iron projected onto the detector axis, thus minimizing any dependence on pulse-height calibration. A minimal projected range of 40 cm was required, ensuring full trigger efficiency in the two detectors. A Monte Carlo simulation showed that this cut had at the same time the effect of reducing the contribution of neutral-current interactions to the event sample to less than 5%. The average energy of the accepted neutrino events is approximately 3 GeV.

After all cuts we were left with $\sim 22,000$ events in the front detector, with a contamination of 50 cosmic-ray events. The corresponding rates in the back detector were ~ 3300 neutrino and 290 cosmic-ray events.

The Monte Carlo simulation was used to correct the ratio of the rates in the two detectors for small differences in the ν spectrum and in the detector geometry. The simulation used measured hadron production and neutrino interaction cross-sections and included all known effects such as secondary proton interactions and hadron absorption in the target, and hadron production in the decay region and in the beam dump^{*)}. Neutrino interactions in the material around the detectors, neutral-current neutrino interactions, and minor differences in the functioning of the two detectors were also taken into account. The typical correction to the geometrical scaling (the ratio of the distances squared divided by the number of fiducial modules) is 5%.

The ratio of rates in the two detectors divided by the ratio of simulated events is

$$(N_{\text{back}}/N_{\text{front}})_{\text{data}}/(N_{\text{back}}/N_{\text{front}})_{\text{MC}} = 1.044 \pm 0.023,$$

and for the modules of type I and II, 1.036 ± 0.028 and 1.059 ± 0.040 , respectively. The errors given here are statistical only. The ratio is expected to be unity in the absence of oscillations and below one for small Δm^2 . For $\Delta m^2 \gtrsim 10 \text{ eV}^2$, however, an analysis in terms of integrated event numbers is no longer sensitive since the expected ratios for oscillations become unity or larger.

More information than that from the integrated event rates can be obtained by looking at the ratio of rates as a function of projected range in iron (see fig. 2). The curves indicate the expected variation of the ratios for different values of Δm^2 and $\sin^2 2\theta$. When there are no oscillations the ratio should be independent of range. The data show no significant sign of an oscillation.

The systematic uncertainties in the experiment were estimated by varying the parameters of the analysis over the expected range of uncertainty and studying the effect on the ratio of events in the two detectors. The most serious contributions came from the dead-time correction, the differences in event reconstruction efficiency and the performance of the two detectors, and the number of events entering from outside the fiducial volume but not identified as such. Each of these uncertainties was estimated to be 1%. The second serious group of uncertainties came from our imperfect knowledge of the hadron production energy and transverse momentum spectra, the hadron absorption in the target, the hadronic spectra from secondary proton interactions, the effect

^{*)} The Monte Carlo simulation agreed well with the results of a test run in which the experimental target was removed and the proton beam was allowed to strike the beam dump.

of proton interactions downstream of the target, and possible trigger inefficiencies. Each of these was estimated to be at most 0.5%. Finally, uncertainties in neutrino cross-sections and the cosmic-ray subtraction were estimated to contribute less than 0.5%. By adding all these contributions in quadrature, the over-all systematic uncertainty in the ratio of event rates in the two detectors was estimated to be 2.5%.

From the event rates in the two detectors as a function of range (fig. 2) and taking a 2.5% systematic uncertainty into account, limits on ν_μ oscillations can be set as a function of $\sin^2 2\Theta$ and Δm^2 , as shown in fig. 3. The area to the right of the curve is excluded at the 90% confidence level. For maximal mixing, Δm^2 values between 0.26 and 90 eV^2 are excluded. The most restrictive limit on the neutrino mixing-angle parameter $\sin^2 2\Theta$ is determined to be 0.053 at $\Delta m^2 = 2.5 \text{ eV}^2$. The limits obtained are the most restrictive ones on $\nu_\mu \leftrightarrow \nu_e$ oscillations [3,5] for $1 \leq \Delta m^2 \leq 3 \text{ eV}^2$, on $\nu_\mu \leftrightarrow \nu_\tau$ oscillations [3,4] for $\Delta m^2 \leq 10 \text{ eV}^2$, and on $\nu_\mu \leftrightarrow \nu_x$ oscillations [7] (ν_x being an unknown species of neutrino) for $\Delta m^2 \leq 20 \text{ eV}^2$.

We would like to thank the staff of the CERN Proton Synchrotron and Experimental Facilities Divisions for their efficient co-operation in setting up and operating the proton beam. We are indebted to our technical collaborators and gratefully acknowledge their competent assistance.

References

- [1] B. Pontecorvo, Zh. Eksp. Teor. Fiz. **53** (1967) 1717 [Sov. Phys.-JETP **26** (1968) 984].
- [2] J. Blietschau et al., Nucl. Phys. **B133** (1978) 205;
H. Deden et al., Phys. Lett. **98B** (1981) 310;
N. Armenise et al., Phys. Lett. **100B** (1981) 182;
O. Erriquez et al., Phys. Lett. **102B** (1981) 73;
A.E. Asratyan et al., Phys. Lett. **105B** (1981) 301.
- [3] N.J. Baker et al., Phys. Rev. Lett. **47** (1981) 1576.
- [4] N. Ushida et al., Phys. Rev. Lett. **47** (1981) 1694.
- [5] $\nu_\mu \rightarrow \nu_e$ oscillations can also be studied by ν_e disappearance experiments. See J.L. Vuilleumier et al., Phys. Lett. **114B** (1982) 298.
- [6] M. Holder et al., Nucl. Instrum. Methods **148** (1978) 235.
- [7] C. Haber et al., Fermilab preprint, FERMILAB-CONF-83/57-EXP (1983).

Figure captions

Fig. 1: Layout of the CDHSW oscillation experiment.

- a) New PS beam line pointing toward the newly built front detector at 130 m and the already existing back detector at 885 m.
- b) Layout of the detectors. The concrete wall in front of the back detector equalizes the environment of muons produced by neutrino interactions in the concrete.

Fig. 2: Ratio of Monte Carlo corrected event rates in the back and front detector as a function of projected range in iron. Events starting in the two types of modules are given separately. Also shown are curves indicating the expected behaviour of these ratios in the case of oscillations for different choices of Δm^2 and $\sin^2 2\theta$. — $\Delta m^2 = 1 \text{ eV}^2$ and $\sin^2 2\theta = 0.2$; - - - $\Delta m^2 = 1 \text{ eV}^2$ and $\sin^2 2\theta = 1$; ···· $\Delta m^2 = 32 \text{ eV}^2$ and $\sin^2 2\theta = 0.2$; ——— $\Delta m^2 = 32 \text{ eV}^2$ and $\sin^2 2\theta = 1$.

Fig. 3: Limits on the oscillation parameters Δm^2 versus $\sin^2 2\theta$:

The solid line is the 90% CL obtained in this experiment. The dashed lines are a compilation of the best limits obtained in earlier experiments: $\nu_\mu \rightarrow \nu_e$ (from ref. 3); $\nu_\mu \rightarrow \nu_\tau$ (from ref. 4); $\nu_\mu \rightarrow \nu_x$ (from ref. 7); $\bar{\nu}_e \rightarrow \bar{\nu}_x$ (from ref. 5).

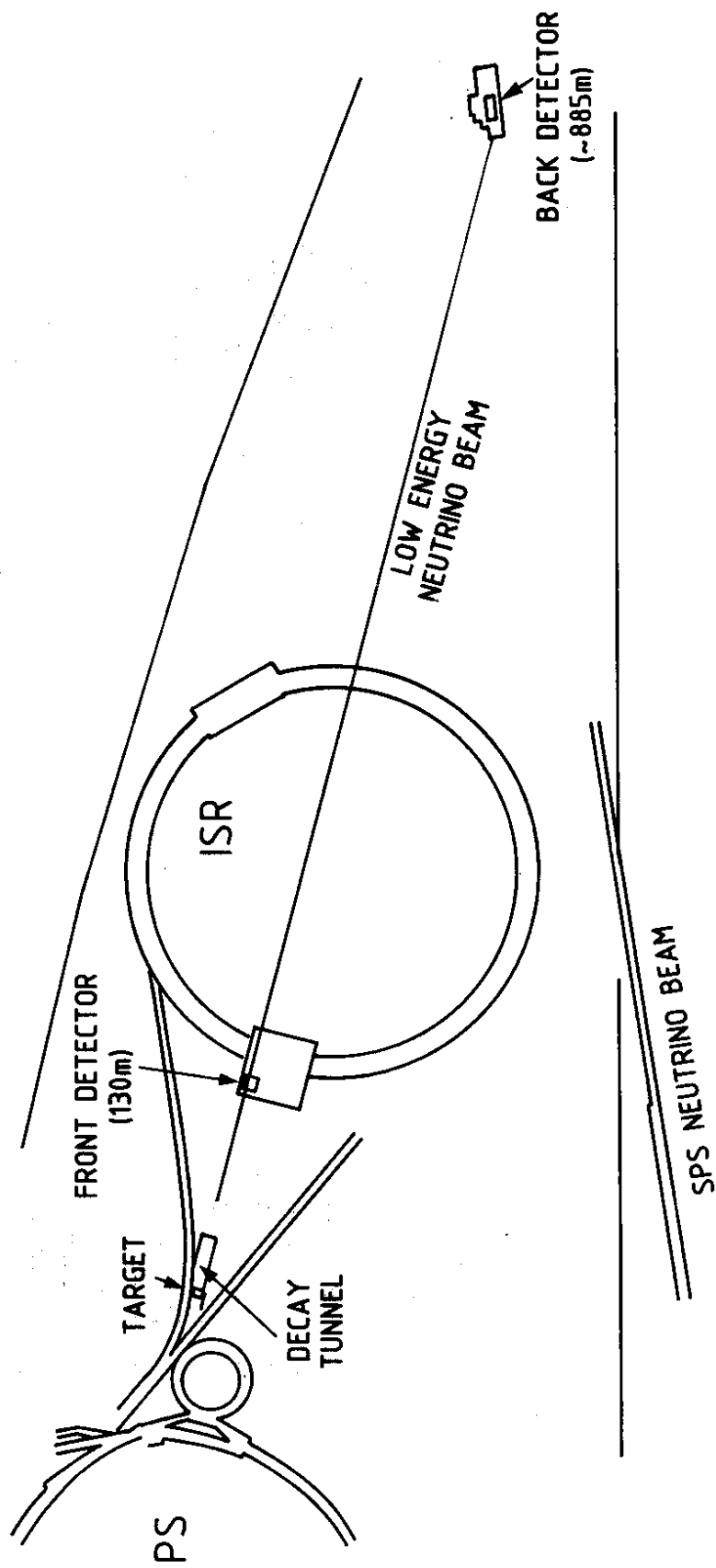
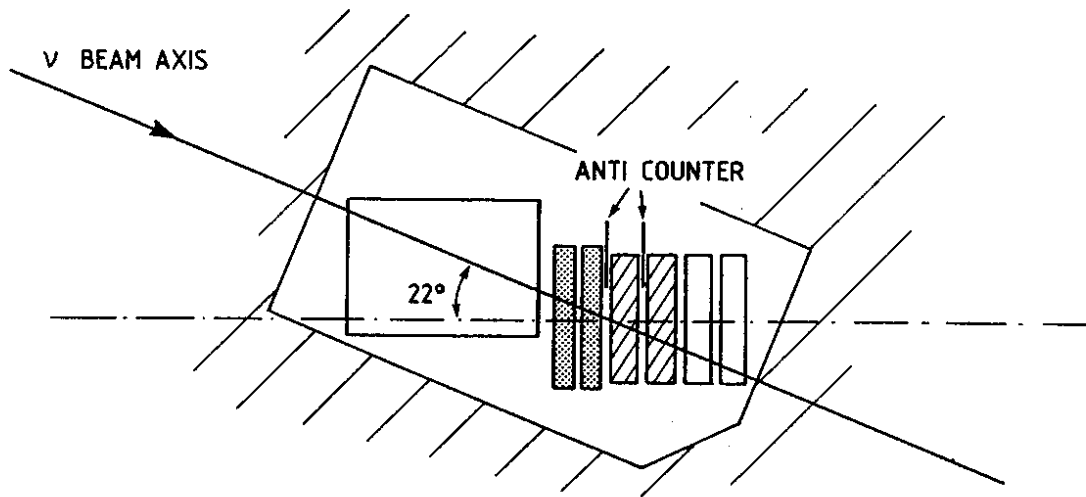


Fig. 1 a)

DETECTOR AT 130m



DETECTOR AT 885m

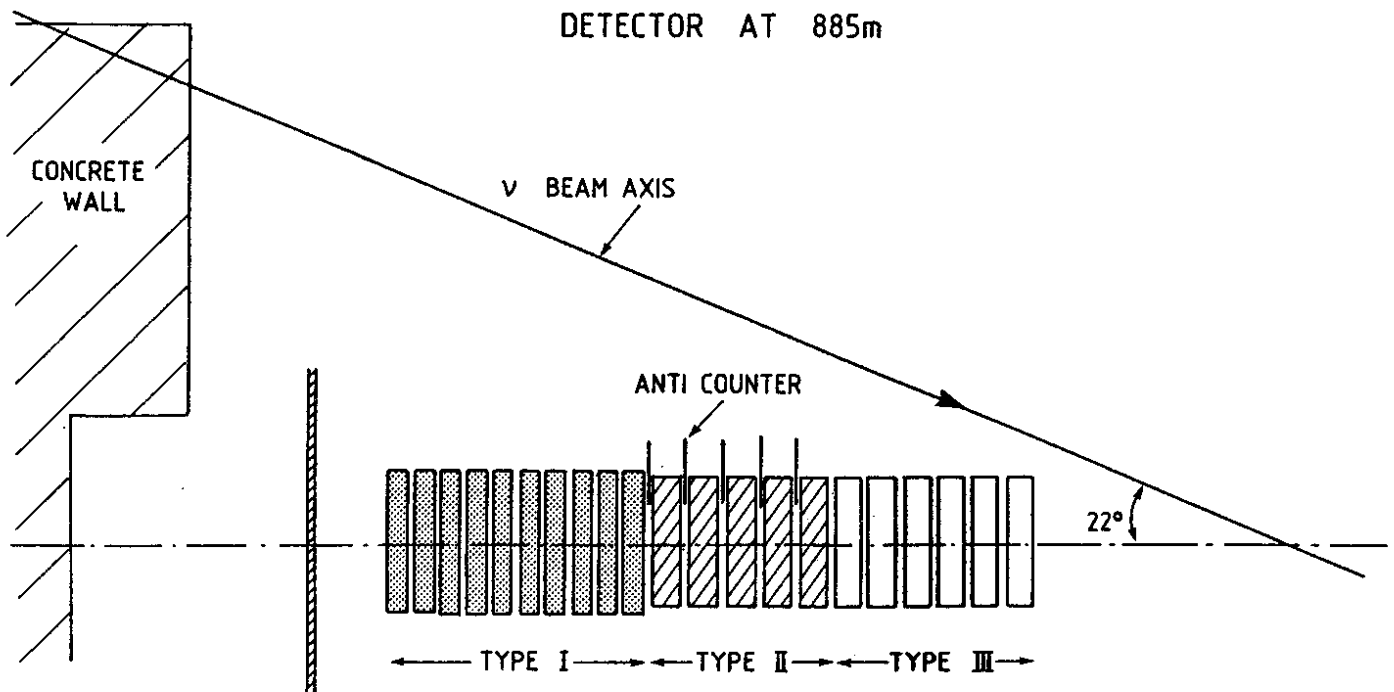


Fig. 1 b)

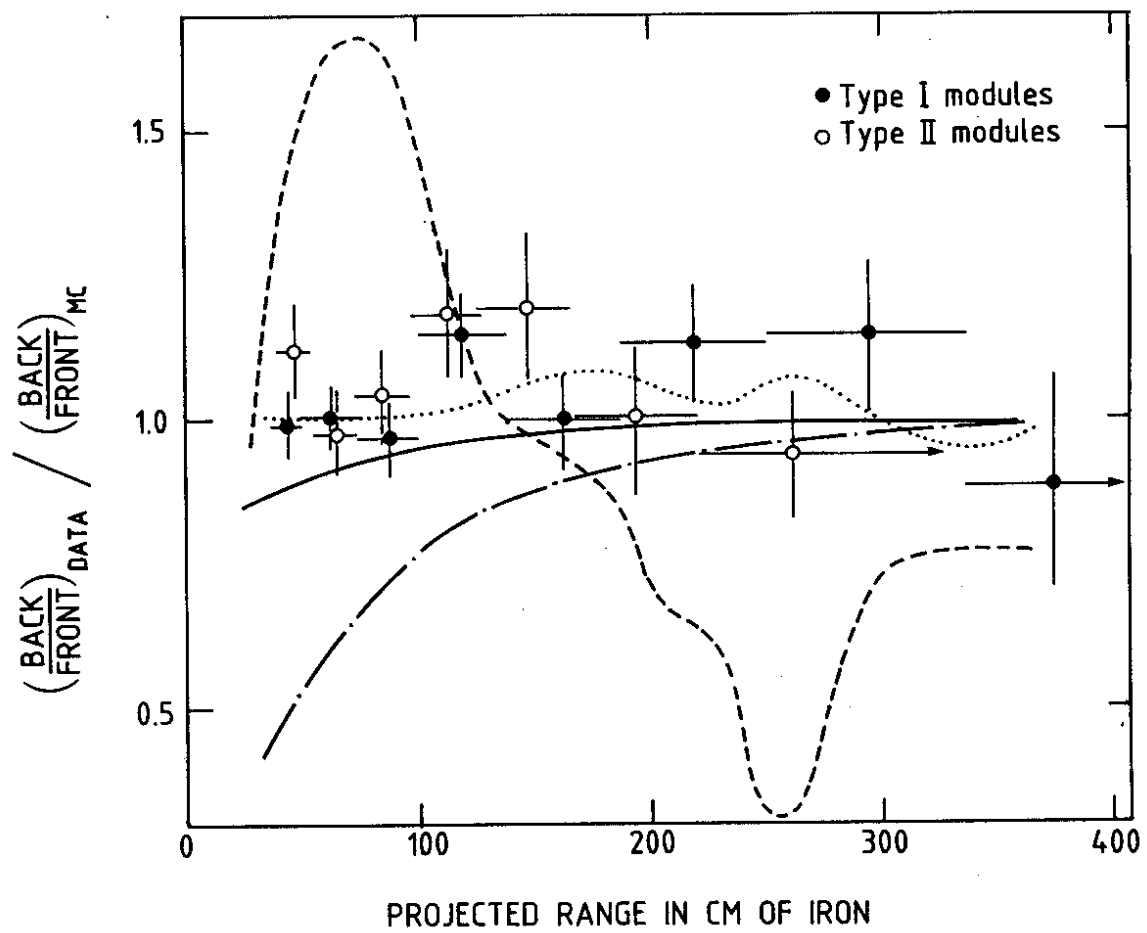


Fig. 2

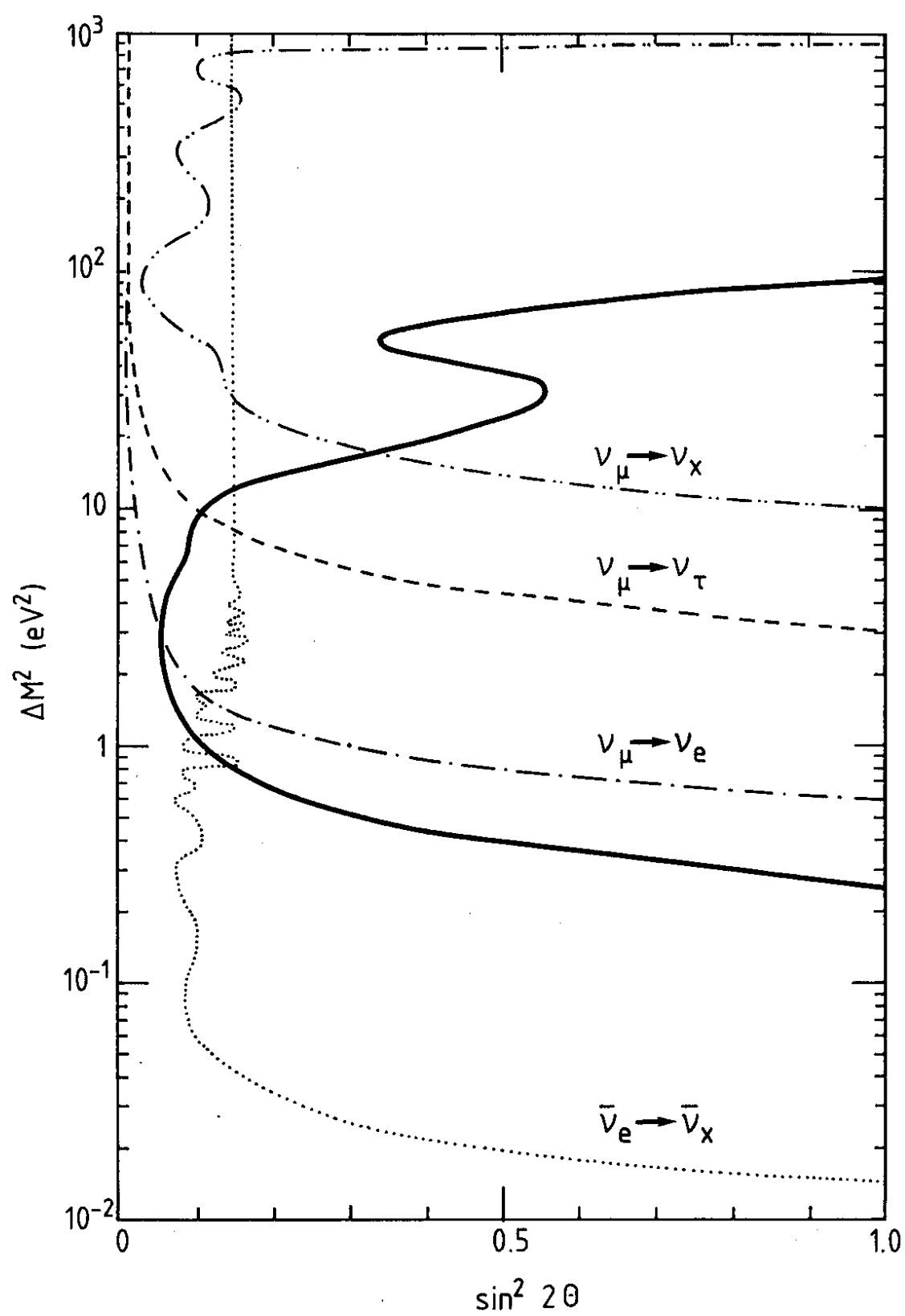


Fig. 3